Kinematic and static analyses of the spherical X-joint: a new cable-driven spherical 4R linkage

Vimalesh Muralidharan[1], Durgesh Haribhau Salunkhe[2], Christine Chevallereau[3], and Philippe Wenger[3]

[1] School of Mechanical Sciences, IIT Bhubaneswar, India {vimalesh@iitbbs.ac.in}
[2] EPFL, Lausanne, Switzerland {Durgesh.Salunkhe@epfl.ch}
[3] Nantes Université, ECN, CNRS, LS2N, Nantes, France
{{Christine.Chevallereau, Philippe.Wenger}@ls2n.fr}

Abstract. This work presents the spherical X-joint, a novel 4R spherical linkage featuring two pairs of identical links arranged in a crossed configuration. A rigorous kinematic analysis reveals that the mechanism exhibits a unique reflective symmetry and that its full-cycle mobility is theoretically equivalent to pure rolling between identical elliptical cones. This insight enables an unconstrained single-parameter description of the joint's motion that extends the inherent symmetry of the mechanism to the mathematical analysis also. Such a description provides a compact and efficient kinematic and static model for the spherical X-joint. Furthermore, a remote actuation strategy based on antagonistic cables is proposed, and it is analytically proven that the joint exhibits positive coactivation across its workspace. These findings demonstrate the spherical X-joint's strong potential for remote actuation applications, particularly in the design of lightweight, bio-inspired robotic wrists and manipulators.

Keywords: Spherical X-joint, mobility, parametrization, coactivation

1 Introduction

A *spherical four-bar linkage* (often called a 4R spherical mechanism) consists of four rigid links connected by revolute joints whose axes intersect at a common center point. This configuration constrains all motion to the surface of a sphere, analogous to how a planar four-bar is constrained to a plane.

The kinematic synthesis of spherical four-bar mechanisms has been studied for decades alongside the planar counterpart [1]. McCarthy's work on the *opposite pole quadrilateral* provided a useful parameterization for these linkage solutions, laying a foundation for computer-aided spherical mechanism synthesis [2]. In bio-inspired mechanisms, spherical four-bars (sometimes in parallelogram form) have been used to mimic ball-and-socket joints - for instance, coordinating the flapping and twisting of a wing segment in a flapping UAV [3]. Another interesting application of spherical four-bar mechanism can be found in the model of a knee joint, where the tibiofemoral complex is represented by

a crossed linkage [4]. In conjunction with the above study, D'Alessio et al. [5] designed a spherical 4R linkage using five poses of the femur bone relative to the tibia bone. They further developed a prosthetic knee with cams in the shape of the fixed and moving axode surfaces of the above linkage.

This paper presents a complete kinematic analysis of the spherical equivalent of the planar X-joint or anti-parallelogram linkage, referred to as the spherical X-joint. The motivation of this work is to design lightweight bio-inspired robotic spherical wrists with large orientation ranges and stiffness tuning capabilities, two interesting features met in the planar X-joint [6]. We propose a remote actuation of the spherical X-joint with two antagonistic cables and prove that it has a positive coactivation factor (see, e.g., [7],[8]). This result shows that the spherical X-joint will be suitable for developing bio-inspired manipulators.

The rest of this paper is organized as follows: Section 2 describes the geometry of the spherical X-joint. Section 3 presents the instantaneous and full-cycle mobility analysis of the spherical X-joint. Section 4 studies the coactivation behavior of the joint while it is remotely actuated by antagonistic cables. Finally, Section 5 presents the conclusions of this work.

2 Mechanism description and kinematic model

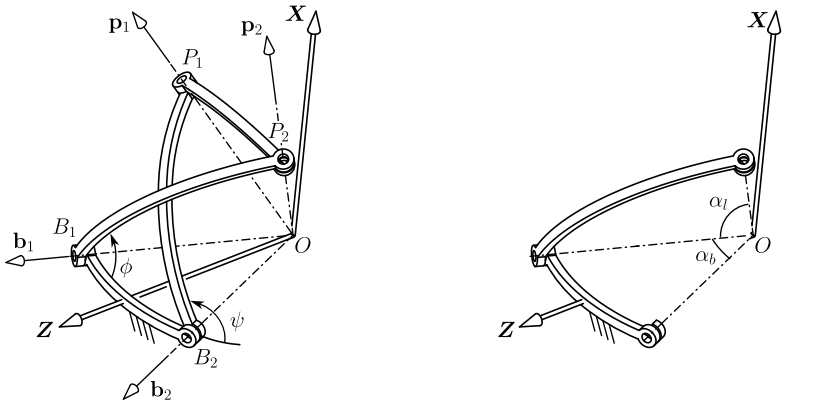

(a) Spherical X-joint. (b) Architecture parameters (α_b, α_l).

Fig. 1: Schematic of the spherical X-joint and its constituent links.

This section describes the spherical X-joint and establishes the relationship between the angular displacement of the two crossed links. Figure 1 presents the schematic of the spherical X-joint. It comprises four links: base link (B_1B_2), top link (P_1P_2), and two crossed links (B_1P_2, B_2P_1). These links are interconnected by four revolute joints to form a closed kinematic chain $(B_1B_2P_1P_2B_1)$ as shown in Fig. 1a. The axes of all the revolute joints pass through a common point O

which results in a spherical mechanism, otherwise called a spherical joint in this paper. The architecture of this joint is defined by four parameters which describe the constant angle subtended by each of the links at the point O. In this article, we consider a special geometry for the spherical joint where the base and top links (resp. two crossed links) have identical architecture defined by the angle α_b (resp. α_l) as shown in Fig. 1b. Since this symmetric architecture resembles the anti-parallelogram mechanism (or X-joint) in a plane, we refer to this joint as the spherical X-joint. In this study, we restrict $\alpha_b, \alpha_l \in]0, \pi[$ and note that $(\alpha_l > \alpha_b)$ is necessary for the assembly of the spherical X-joint.

Without loss of generality, we define the points B_1, B_2, P_1, P_2 on a unit sphere centered at O on their respective revolute axes. Let $\mathbf{b}_1, \mathbf{b}_2, \mathbf{p}_1, \mathbf{p}_2$ represent the unit vectors along the four revolute axes as shown in Fig. 1a. The coordinates (ϕ, ψ) represent the angular displacement[1] of the two crossed links relative to the base about the axes $(\mathbf{b}_1, \mathbf{b}_2)$, respectively. The unit vectors above can be expressed in terms of the architecture parameters (α_b, α_l) and the angle coordinates (ϕ, ψ), in the reference frame O-$\boldsymbol{XYZ}$ (see Fig. 1a), as follows:

$$\mathbf{b}_1 = \begin{bmatrix} 0 \\ s_{b_2} \\ c_{b_2} \end{bmatrix}, \mathbf{b}_2 = \begin{bmatrix} 0 \\ -s_{b_2} \\ c_{b_2} \end{bmatrix}, \mathbf{p}_1 = \begin{bmatrix} s_\psi\, s_l \\ -c_{b_2}\, c_\psi\, s_l - s_{b_2}\, c_l \\ -s_{b_2}\, c_\psi\, s_l + c_{b_2}\, c_l \end{bmatrix}, \mathbf{p}_2 = \begin{bmatrix} s_\phi\, s_l \\ s_{b_2}\, c_l - c_{b_2}\, c_\phi\, s_l \\ s_{b_2}\, c_\phi\, s_l + c_{b_2}\, c_l \end{bmatrix} \quad (1)$$

where $s_{b_2} = \sin\left(\frac{\alpha_b}{2}\right)$, $c_{b_2} = \cos\left(\frac{\alpha_b}{2}\right)$, $s_l = \sin\alpha_l$, $c_l = \cos\alpha_l$, $s_\phi = \sin\phi$, $c_\phi = \cos\phi$, $s_\psi = \sin\psi$, $c_\psi = \cos\psi$. The loop-closure equation to relate ϕ with ψ can be obtained through the rigidity condition of the top link, i.e., specifying the angle between $\mathbf{p}_1$ and $\mathbf{p}_2$ as α_b:

$$\mathbf{p}_1 \cdot \mathbf{p}_2 = \cos\alpha_b \implies s_l(c_\psi c_\phi - 1)c_b + s_b c_l c_\phi - s_b c_l c_\psi + s_\psi s_l s_\phi = 0 \quad (2)$$

where $c_b = \cos\alpha_b, s_b = \sin\alpha_b$. This equation can be rearranged in the form:

$$A_\psi \cos\psi + B_\psi \sin\psi + C_\psi = 0 \quad (3)$$

where $A_\psi = c_\phi c_b s_l - c_l s_b, B_\psi = s_\phi s_l, C_\psi = c_l c_\phi s_b - s_l c_b$. It is well-known that the above equation has two solutions for ψ for every given ϕ. They correspond to the non-crossed and crossed configurations for the limbs, akin to the parallelogram and anti-parallelogram configurations in a planar setting. Since this study focuses on the crossed configurations of the limbs only, we choose the respective solution branch as follows:

$$\cos\psi = \frac{-A_\psi C_\psi - B_\psi\sqrt{A_\psi^2 + B_\psi^2 - C_\psi^2}}{A_\psi^2 + B_\psi^2}, \sin\psi = \frac{-B_\psi C_\psi + A_\psi\sqrt{A_\psi^2 + B_\psi^2 - C_\psi^2}}{A_\psi^2 + B_\psi^2} \quad (4)$$

This choice is valid while the spherical X-joint operates within its flat-singularities, i.e., $\phi, \psi \in]0, \pi[$.

[1] The angular displacement ϕ of a crossed link B_1P_2 relative to the base B_1B_2 refers to the angle between the planes B_1OP_2 and B_1OB_2 (or their respective normal directions) measured in the counterclockwise sense about the unit vector $\mathbf{b}_1$.

3 Instantaneous and full-cycle mobility

The instantaneous and full-cycle mobility of the spherical X-joint are detailed in the following sections.

3.1 Instantaneous mobility

Let the points B and P denote the mid-points of the arcs B_1B_2 and P_1P_2, respectively, as illustrated in Fig. 2. We observe that the spherical X-joint under study consists of two kinematic chains, namely the BB_1P_2P chain and the BB_2P_1P chain. Each chain comprises two revolute joints, whose axes pass through the center point O. For the BB_1P_2P chain, the first revolute joint axis passes through points B_1 and O, while the second passes through P_2 and O. These two axes together constrain the motion of the mechanism such that the resulting instantaneous degree of freedom is a pure rotation about an axis passing through O and lying within the plane formed by points B_1, P_2, and O (refer to the red plane in Fig. 2). An analogous description holds for the BB_2P_1P chain, with its instantaneous rotation axis constrained to pass through O and lie in the plane defined by B_2, P_1, and O (refer to the blue plane in Fig. 2).

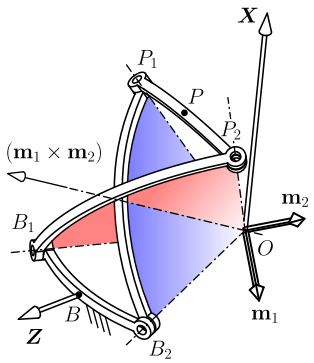

Fig. 2: The instantaneous axis of rotation of the spherical X-joint.

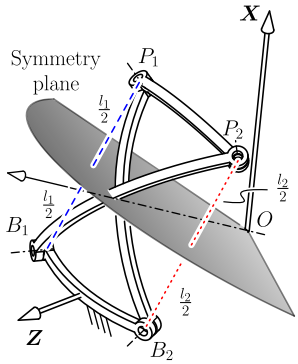

Fig. 3: The symmetry plane of the spherical X-joint.

Consequently, the overall instantaneous mobility of the mechanism is characterized by a single rotation about the axis formed by the intersection of these two planes. This instantaneous axis of rotation can be identified by taking the cross product of the normals to each plane ($\mathbf{m}_1$ and $\mathbf{m}_2$) as shown in Eq. (5).

$$\mathbf{m}_1 = \begin{bmatrix} c_\phi \\ c_{b_2}\, s_\phi \\ -s_{b_2}\, s_\phi \end{bmatrix}, \mathbf{m}_2 = \begin{bmatrix} c_\psi \\ c_{b_2}\, s_\psi \\ s_{b_2}\, s_\psi \end{bmatrix}, \mathbf{m}_1 \times \mathbf{m}_2 = \begin{bmatrix} s_b\, s_\phi\, s_\psi \\ -s_{b_2}\, c_{\phi-\psi} \\ c_{b_2}\, c_{\phi+\psi} \end{bmatrix} \tag{5}$$

where $c_{\phi-\psi} = \cos(\phi - \psi)$ and $c_{\phi+\psi} = \cos(\phi + \psi)$.

3.2 Full-cycle mobility

Reflective symmetry in the spherical X-joint

In this subsection, we formally establish the existence of a reflective symmetry plane within the mechanism. To begin with, we use the fact that in three-dimensional space, two distinct rays emanating from a common point have a unique plane of reflective symmetry.

In the mechanism under consideration, the vectors $\mathbf{b}_1$ and $\mathbf{p}_1$ have a plane of symmetry passing through the origin. The normal vector to this symmetry plane can be determined as the vector from B_1 to P_1, denoted by $\overrightarrow{B_1P_1}$.

Similarly, the vectors $\mathbf{b}_2$ and $\mathbf{p}_2$ have another plane of symmetry that passes through the origin with its normal vector given by $\overrightarrow{B_2P_2}$. To verify whether these two symmetry planes are identical, we consider the cross product of the two vectors as follows:

$$\overrightarrow{B_2P_2} \times \overrightarrow{B_1P_1} = \begin{bmatrix} (-c_l(c_\phi - c_\psi)c_b + s_l(c_\psi c_\phi - 1)s_b + c_\phi - c_\psi)\, s_l \\ s_l\,(-(c_l - 1)(s_\phi - s_\psi)c_{b_2} + s_l s_{b_2}(s_\psi c_\phi + c_\psi s_\phi)) \\ (-(c_l + 1)(s_\phi + s_\psi)s_{b_2} + s_l c_{b_2}(s_\psi c_\phi - c_\psi s_\phi))\, s_l \end{bmatrix} \tag{6}$$

We verified that the above vector evaluates to null, when we incorporate the relation involving ϕ and ψ from Eq. (4). Thus, the two symmetry planes coincide, leading to a symmetry in the entire mechanism.

As B_1 is symmetric to P_1, and B_2 is symmetric to P_2 with respect to the reflective plane of symmetry, the crossed-limbs B_1P_2 and B_2P_1 are also symmetric about the same plane. Consequently, the planes B_1OP_2 and B_2OP_1 are symmetric with respect to the reflective symmetry plane passing through the origin (refer to gray plane in Fig. 3). Therefore, the intersection line of the planes B_1OP_2 and B_2OP_1 lies on the symmetry plane. Since the instantaneous axis of rotation of the mechanism is determined by the intersection of these two planes, it follows that the instantaneous axis of rotation lies on the symmetry plane too.

Axodes of the spherical X-joint

In a planar anti-parallelogram mechanism, it is established that the relative motion between the base and coupler links is equivalent to pure rolling between two centrodes in the form of identical ellipses [9, pp. 115-117]. On the other hand, in a spherical mechanism, the relative motion between the base and coupler links is equivalent to pure rolling between two ruled surfaces (fixed and moving axodes) [10]. For the spherical X-joint, the fixed axode can be determined by using planes B_1OP_2 and B_2OP_1 given as $\mathbf{m}_1 \cdot \mathbf{x} = 0$, and $\mathbf{m}_2 \cdot \mathbf{x} = 0$ respectively, where $\mathbf{x} = [x, y, z]^T$ denotes a generic point in space. Using the loop closure condition of the mechanism given in Eq. (2) and eliminating the variables ϕ and ψ, we obtain two algebraic equations that define the fixed axode. Geometrically, these equations describe two elliptical cones with their apex at the origin and axis aligned with the z-axis. One of these elliptical cones corresponds to the crossed configuration for the limbs of the mechanism, while the other corresponds to

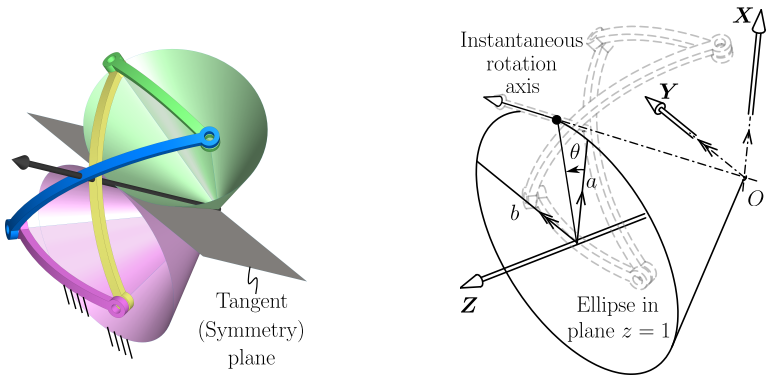

(a) Pure rolling of two elliptical cones. (b) Parametrization of the full-cycle motion of the spherical X-joint.

Fig. 4: Kinematic equivalence of the spherical X-joint as pure rolling of symmetrically placed identical elliptical cones, and motion parameterization.

non-crossed configuration. The equation of the elliptical cone associated with the crossed configuration or the spherical X-joint is the following:

$$\frac{x^2}{a^2} + \frac{y^2}{b^2} = z^2, \text{ where, } a = \sqrt{\frac{s_{l_2}^2 - s_{b_2}^2}{c_{l_2}^2}}, b = \sqrt{\frac{s_{l_2}^2}{c_{l_2}^2}} \tag{7}$$

where $a, b > 0$ represent the semi-minor and semi-major axes lengths of the ellipse in the plane $z = 1$. From the above expressions, it is clear that $a < b$, which indicates that the ellipse is aligned such that its major (resp. minor) axis is along the y-axis (resp. x-axis).

To determine the moving axode, it is necessary to fix the coupler link of the spherical X-joint and analyze the resulting motion relative to the coupler frame. As discussed in the previous subsection, the mechanism exhibits a reflective plane of symmetry that passes through the origin. Furthermore, the instantaneous axis of rotation lies on this symmetry plane. Due to this symmetry, the moving axode is obtained as the mirror image of the fixed axode across the plane of symmetry, as illustrated in Fig. 4a.

This symmetry relation between the fixed and moving axodes provides valuable insights related to the kinematic equivalence of the spherical X-joint as pure rolling of an elliptical cone on another as shown in Fig. 4a. A motion simulation of the spherical X-joint along with the associated elliptical cones can be found in this link[2].

[2] https://youtu.be/uqjcHYIQXfs

3.3 Motion parametrization

As the axode is an elliptical cone with its axis directed along the z-axis, we obtain an ellipse in the plane $z = 1$ as shown in Fig. 4b. The points on this ellipse can be parametrized with a single parameter θ, which also represents a generator of the elliptical cone (refer to Fig. 4a). The generator of the elliptical cone is also the instantaneous axis of rotation, and thus, the configuration of the spherical X-joint can be uniquely determined by θ. Using this coordinate to describe the pose of the coupler link provides an unconstrained description of its motion, unlike other coordinates (ϕ, ψ) which must be used along with the loop-closure equation. Another advantage of using θ is that it reflects the inherent symmetry of linkage: $\theta = 0$ is the home configuration for all architectures of the spherical X-joint; $\pm\theta$ depict the same angular tilt of the coupler link in the counter-clockwise and clockwise directions, respectively.

The plane of symmetry of the spherical X-joint can be expressed in terms of θ as follows:

$$\frac{\cos\theta}{a}x + \frac{\sin\theta}{b}y - z = 0 \tag{8}$$

4 Cable actuation and coactivation

In this section, we consider the remote actuation of the spherical X-joint with cables and study its stiffness modulation properties. The two antagonistic cables actuating the joint are attached between the points (B_1, P_1) and (B_2, P_2) as shown in Fig. 3 in blue dashed and red dotted lines, respectively. The length of these cables, denoted by l_1, l_2, can be computed as twice the distance of the points B_1, B_2 from the plane of symmetry, respectively. Using Eqs. (1) and (8), they can be expressed in terms of θ as:

$$l_1 = \frac{2a(bc_{b_2} - s_{b_2}\sin\theta)}{\sqrt{b^2\cos^2\theta + a^2\sin^2\theta + a^2b^2}}, \quad l_2 = \frac{2a(bc_{b_2} + s_{b_2}\sin\theta)}{\sqrt{b^2\cos^2\theta + a^2\sin^2\theta + a^2b^2}} \tag{9}$$

Since the spherical X-joint is a 1-DoF system actuated by two cables, there is an actuation redundancy of order 1. This redundancy can be used to modulate the stiffness of the joint in any configuration. In biological systems, agonist-antagonist muscles or muscle groups work synchronously to achieve this stiffness modulation. By default, the muscles are relaxed and the joint exhibits low stiffness, but when both muscle groups are activated simultaneously, the joint exhibits high stiffness, known as coactivation [11]. This is an energy-efficient and natural way to modulate stiffness. In our previous work, we studied several single-DoF planar joints for the coactivation property [12]. In this study, we will investigate if the spherical X-joint exhibits coactivation or not.

The correlation between actuation forces and joint stiffness is characterized by the coactivation factor [7],[8], which is defined in terms of the first- and second-order derivatives of the cable lengths as:

$$\gamma_1 = \frac{\mathrm{d}^2 l_1}{\mathrm{d}\theta^2} - \frac{(\mathrm{d}l_1/\mathrm{d}\theta)}{(\mathrm{d}l_2/\mathrm{d}\theta)}\frac{\mathrm{d}^2 l_2}{\mathrm{d}\theta^2} \tag{10}$$

If the coactivation factor is positive, the joint stiffness can be increased by increasing the actuation forces, similar to that of a biological joint [8]. From Eq. (9), the coactivation factor of the spherical X-joint is found to be:

$$\gamma_1 = \frac{4ab^2\left(b^2-a^2\right)\left(a^2+1\right)c_{b_2}s_{b_2}\cos^2\theta}{\left(b^2\cos^2\theta + a^2\sin^2\theta + a^2b^2\right)^{3/2}\left(\nu(\theta)\right)}, \text{ where,}$$
$$\nu(\theta) = \left(-a^2+b^2\right)c_{b_2}\sin\theta + \left(a^2b+b\right)s_{b_2} \tag{11}$$

Recalling that $b > a > 0$ (see Section 3.2) and $\alpha_b \in]0, \pi[$ (see Section 2), it is apparent that all the factors in the numerator and denominator of γ_1, except $\nu(\theta)$, are positive. Hence, the sign of γ_1 depends solely on the sign of $\nu(\theta)$.

Let us consider the lower bound of $\nu(\theta)$ obtained by setting $\sin\theta = -1$:

$$\underline{\nu} = -\left(-a^2+b^2\right)c_{b_2} + \left(a^2b+b\right)s_{b_2} \tag{12}$$

Upon substituting the expressions of a and b from Eq. (7) and simplifying the result, one obtains:

$$\underline{\nu} = \frac{s_{b_2}c_{b_2}\sin\left(\frac{\alpha_l-\alpha_b}{2}\right)}{c_{l_2}^3} \tag{13}$$

Recalling from Section 2 that $(\alpha_l > \alpha_b)$ is an assembly condition for the spherical X-joint, it follows that $\underline{\nu} > 0$. Hence, $\nu(\theta)$ must be positive for all $\theta \in \mathbb{R}$, which implies that γ_1 also remains positive throughout the range of motion. This shows that the spherical X-joint exhibits coactivation, similar to that of a planar X-joint when the cables are connected between the unconnected pivot pairs. Hence, it can be used to develop bio-inspired robots that exhibit coactivation.

5 Conclusions

This paper presented the kinematics of a special 4-revolute spherical linkage, namely, the spherical X-joint, in which the opposite links have identical geometry. Firstly, it was established that there is a unique plane about which the base and coupler links (resp. the two crossed limbs) exhibit reflective symmetry. Secondly, it was shown that the full-cycle mobility of the spherical X-joint is equivalent to pure rolling between two identical elliptical cones. Using this motion description, it was possible to use the parametric form of a planar ellipse to parametrize the configurations of the spherical X-joint, in an unconstrained manner. Finally, a remote actuation scheme for the spherical X-joint was considered with antagonistically arranged cables. It was shown that this joint exhibits positive coactivation, similar to that of a biological joint. Hence, the spherical X-joint can be used to develop new lightweight bio-inspired manipulators.

As a future work, one or more spherical X-joints will be used to develop new robotic wrists and will be compared with the existing 3-revolute architectures.

References

1. D. A. Ruth, J. M. McCarthy, The design of spherical 4R linkages for four specified orientations, Springer Berlin Heidelberg, 1998, pp. 53–67. doi:10.1007/978-3-662-03729-4_3.
2. J. Dooley, J. M. McCarthy, Sphinx: Software for synthesizing spherical 4R mechanisms, in: NSF design and manufacturing systems conference, 1993.
3. S. O'Connor, M. Plecnik, The synthesis of spherical four-bars for biomimetic motion through complete solutions for approximate rigid body guidance, Journal of Mechanisms and Robotics 17 (4) (2025) 044517. doi:10.1115/1.4066850.
4. N. Sancisi, V. Parenti-Castelli, A novel 3D parallel mechanism for the passive motion simulation of the patella-femur-tibia complex, Meccanica 46 (2011) 207–220. doi:10.1007/s11012-010-9405-x.
5. J. D'Alessio, K. Russel, R. S. Sodhi, Spherical four-bar motion generation and axode generation in cam mechanism design, Journal of Advanced Mechanical Design, Systems, and Manufacturing 10 (2016) 1600057. doi:10.1299/jamdsm.2016jamdsm0028.
6. M. Furet, P. Wenger, Kinetostatic analysis and actuation strategy of a planar tensegrity 2-X manipulator, Journal of Mechanisms and Robotics 11 (6) (2019). doi:10.1115/1.4044209.
7. C. Chevallereau, P. Wenger, A. Abourachid, A new bio-inspired joint with variable stiffness, in: International Workshop on New Trends in Medical and Service Robots (MESROB 2023), 2023, pp. 220–227. doi:10.1007/978-3-031-32446-8_24.
8. V. Muralidharan, C. Chevallereau, P. Wenger, Coactivation in symmetric four-bar mechanisms antagonistically actuated by cables, Journal of Mechanisms and Robotics 17 (1) (2025) 010902. doi:10.1115/1.4064981.
9. R. S. Hartenberg, J. Denavit, Kinematic Synthesis of Linkages, McGraw-Hill, 1964.
10. R. Sodhi, T. Shoup, Axodes for the four-revolute spherical mechanism, Mechanism and Machine Theory 17 (3) (1982) 173–178. doi:10.1016/0094-114X(82)90001-5.
11. M. L. Latash, Muscle coactivation: definitions, mechanisms, and functions, Journal of Neurophysiology 120 (2018) 88–104. doi:10.1152/jn.00084.2018.
12. V. Muralidharan, N. Testard, C. Chevallereau, A. Abourachid, P. Wenger, Variable stiffness and antagonist actuation for cable-driven manipulators inspired by the bird neck, Journal of Mechanisms and Robotics 15 (2023) 035002. doi:10.1115/1.4062302.